

Fault imaging of Hibernia 3-D seismic data using edge-detection and coherency measures

Nicholle Carter and Laurence R. Lines

ABSTRACT

“Coherency cube” and fault detection technologies have evolved rapidly in recent years as important tools for seismic interpretation. The following paper, developed as a joint project between investigators at Memorial University and the University of Calgary, compares several of the fault detection methods for data from Hibernia field. The results, which are outlined in detail in the Memorial University M.Sc. thesis of Nicholle Carter, support the usefulness of coherency measures prescribed by Marfurt et al. (1998).

INTRODUCTION

The development of the “coherence cube” and related technologies during recent years has proven to be a valuable interpretive aid for fault detection as evidenced by Nissen et al. (1999). Following the introduction of *The Coherence Cube* by Bahorich and Farmer (1995) for the interpretation of 3-D seismic data from offshore Trinidad, several papers have described the development and application of algorithms for detecting fault discontinuities. One of these, the paper by Marfurt et al. on *3-D seismic attributes using a semblance-based coherency algorithm* received the award for Best Paper in Geophysics in 1998, a testimony to the importance of this technology.

The detection of faults in offshore seismic exploration has been enhanced by use of algorithms from two families – those that measure coherency and those that detect discontinuities or “edges” by differencing. (Actually it is more accurate to say that these algorithms reveal a *lack of coherency* in order to detect faults.) In this study, we apply such “uncoherency” methods to depth migrations from Hibernia field and we compare results for both synthetic and real data. More details of our study are found in the recent M.Sc. thesis of Nicholle Carter of Memorial University of Newfoundland (accepted, September 1999).

HIBERNIA GEOLOGY

Seismic methods play a key role in exploration and reservoir characterization of offshore Newfoundland’s Hibernia oil field, potentially one of North America’s most important offshore sources of crude oil. Figure 1 gives the geographic location of the field on the East Coast of Canada. As shown in Figure 1, Hibernia field, located about 315 km southeast of St. John’s, Newfoundland, is part of the Jeanne d’Arc Basin which includes a large number of extensional faults. A detailed geological picture of this basin is being developed with the use of 3-D seismic surveys. A Hibernia 3-D seismic survey was made available to the Memorial University Seismic Imaging Consortium (MUSIC) by the Hibernia Management and Development Corporation (HMDC) for research into imaging algorithms.

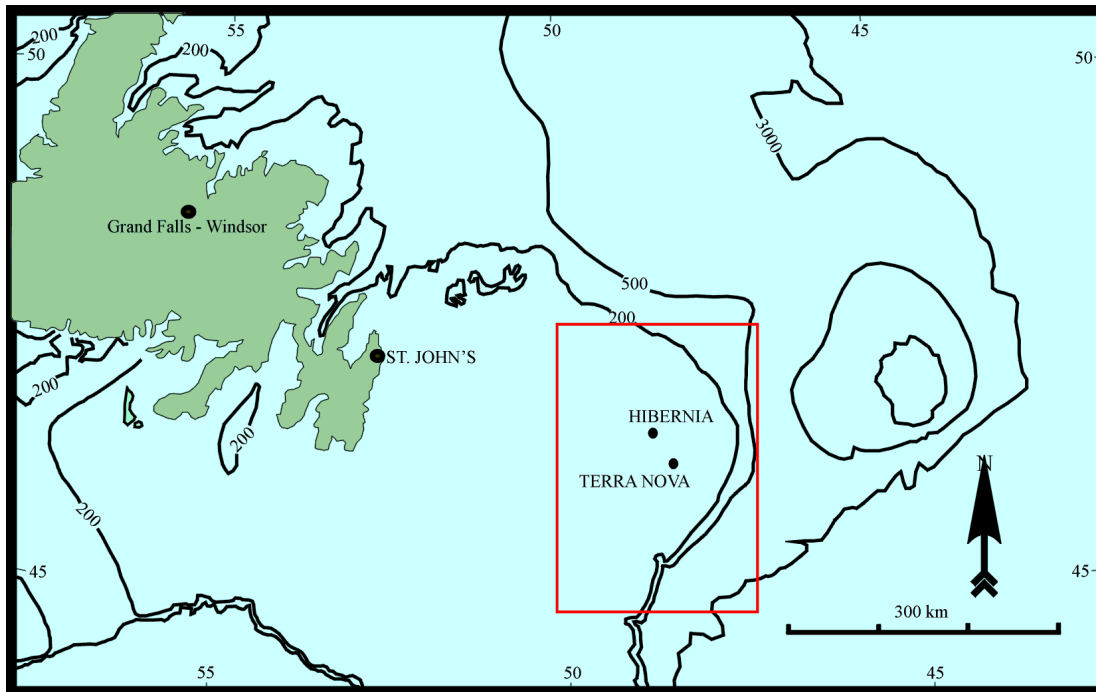


Figure 1. Geographical location of the Hibernia field.

With the development of digital processing methods, it has become possible to extract important geological information from these seismic data, which are traditionally processed to image continuous reflections rather than to image discontinuities such as faults. Thus, when interpreting 3-D seismic data it is often difficult to obtain a clear and unbiased view of faults. Due to the complex structure of offshore Newfoundland fields (Figure 2), fault imaging is extremely important since field production may be affected by sealing faults (Hurley et al., 1992). It is imperative that we accurately image faults within the Hibernia structures for the purposes of enhanced hydrocarbon production and development.

The Hibernia structure is characterized by extensional faulting and a rollover anticline that was formed due to salt diapirism. The Murre fault is a major listric growth fault that bounds the western side of the field (Figure 2). It is offset by the Nautilus fault, which extends along the northeast boundary of the field. The Hibernia field is dissected by a series of smaller faults, which in turn dissect the field into a number of separate blocks via transfer faults. Several small-scale faults have a major effect on the thickness of stratigraphic units. The current strategy for field depletion will be on a block-by-block basis, assuming faults are sealing the hydrocarbons.

METHODOLOGY

The main objective of our study is to compare fault detection methods for 3-D seismic data from the Hibernia field. Our search for optimum fault detection algorithms for Hibernia field had a number of choices, since progress in this field has advanced rapidly in recent years. Following the initial applications presented by Bajorich and Farmer (1995), companies have produced various algorithms for enhanced fault detection. The edge detection method, as presented by Luo et al.

(1996), measures changes in the subsurface such as faults by using differencing of adjacent seismic traces. Marfurt et al. (1998) described the details of algorithms used by Bahorich and Farmer (1995), namely the C1 coherency method, which uses cross-correlation between seismic traces, and the C2 coherency method which uses the semblance measure. Gersztenkorn and Marfurt (1996) extended these methods by developing the C3 algorithm, which used eigenvalues of the covariance matrix in order to produce improvements over the C1 and C2 algorithms. A comparison of the C1, C2, and C3 algorithms was given by Marfurt et al. (1999). In addition to these recently published methods, we examine second derivative methods, which are similar to those used in analysis of potential field data, and which are related to the differencing algorithms of Luo et al.

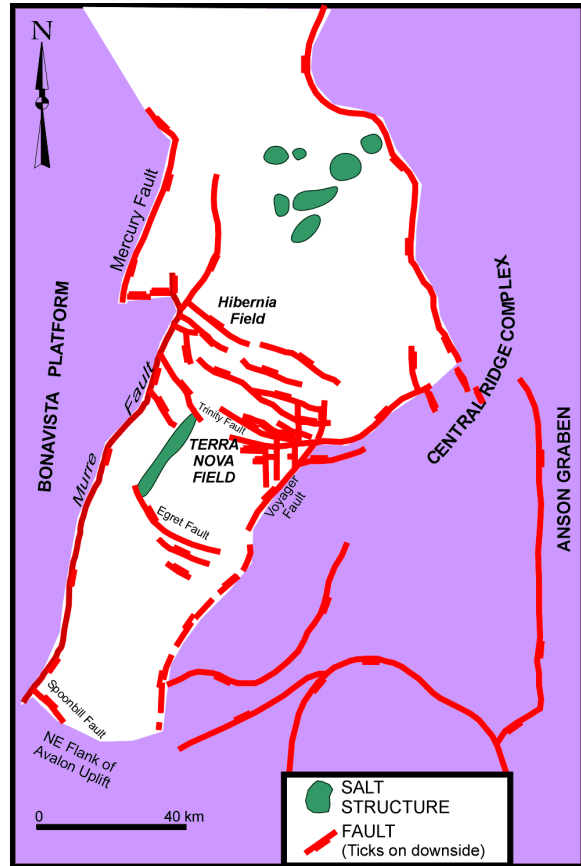


Figure 2. Detailed structure of the Hibernia field.

In this study we mainly compare the C1 algorithm to the differencing method and the second derivative method, although some comparisons with the C2 algorithm are given in the M.Sc. thesis of Carter (1999). For a comparison of the C1, C2 and C3 coherency algorithms, we refer the reader to Marfurt et al. (1999). In our comparisons on the Hibernia data sets, we chose a representative of the data volume containing one or two of the main interpreted faults, and compared the results of the different algorithms. Before examining these results, we briefly describe the mathematics of the algorithms studied here.

Seismic imaging of discontinuities is a relatively new geophysical technique. We compare two main families of algorithms, coherency (Bahorich and Farmer, 1995 and Marfurt et al., 1998, 1999) and differencing (Luo et al., 1996). Both of these algorithms image discontinuities using different mathematical techniques. The C1 coherency algorithm utilizes cross-correlation, $\rho(t)$, between two seismic signals, \vec{A} and \vec{B} , and is shown mathematically to be:

$$\rho(t) = \sum_{\tau} A_{t+\tau} B_{\tau} \tag{1}$$

where A and B are vectors containing seismic trace time sequences $\vec{A} = (A_0, A_1, A_2, \dots, A_n)$ and $\vec{B} = (B_0, B_1, B_2, \dots, B_n)$, and where t is the displacement of \vec{B} relative

to \bar{A} . The C1 algorithm computes the crosscorrelation of traces in the x direction, denoted by ρ_x and the crosscorrelation of traces in the y direction, denoted by ρ_y . The C1 algorithm normalizes these crosscorrelations with respect to trace energies and then computes the maximum values for lags in the x and y directions. The coherency measure ρ_{xy} , is given by the square root of these maximum values, that is, $\rho_{xy} = \sqrt{\max(\rho_x) * \max(\rho_y)}$.

The difference method is a simpler technique which subtracts seismic signals (signal A on the target trace and signal B on an adjacent trace) and is given by:

$$\bar{d} = \frac{\bar{A} - \bar{B}}{|\bar{A}| + |\bar{B}|} \quad (2)$$

where \bar{d} is the difference at the center sample of the window on the target trace (Luo et al., 1996). In our version of the differencing algorithm we average the absolute differences of a grid point and its neighbors. As we will see, the differencing method is somewhat similar to the use of second derivative computations that are used to enhance high wavenumber variations in data.

There is a close relationship between the differencing method of Luo et al. (1996) and the second derivative method used in potential field mapping, as described by Dobrin (1976). This relationship can be shown by use of finite differencing of trace values on a grid. Recall that in analysing potential fields, Laplace's equation gives:

$$\frac{\partial^2 U}{\partial x^2} + \frac{\partial^2 U}{\partial y^2} + \frac{\partial^2 U}{\partial z^2} = 0 \quad (3)$$

where U is the potential field variation.

Therefore, an analysis of

$$\frac{\partial^2 U}{\partial x^2} + \frac{\partial^2 U}{\partial y^2} = -\frac{\partial^2 U}{\partial z^2} \quad (4)$$

is useful for interpreting discontinuities and recognizing the relationship of horizontal changes to vertical changes. Since horizontal second derivative maps in potential field mapping are useful for detecting discontinuities, we consider its possible application to seismic wavefields.

The wave equation would replace the potential, U , by the seismic wavefield, u , and would have an extra term, $\frac{1}{v^2} \frac{\partial^2 u}{\partial t^2}$, on the right hand side of the above equation

where v is seismic velocity and t is time. The second derivative of the wavefield can also be analysed by finite-differences. Consider the wavefield at some particular time slice and at some specific map location at grid point (i,j) . Denote this wavefield value

at some given time by $u_{i,j}$. If h is the grid size and we use second order differencing, the second derivative in the x direction is given by:

$$\frac{\partial^2 u}{\partial x^2} = \frac{1}{h^2}(u_{i+1,j} + u_{i-1,j} - 2u_{i,j}) \quad (5)$$

and similarly for the second derivative in the y direction. Therefore, the Laplacian for variation in the x and y directions is given by:

$$\frac{\partial^2 u}{\partial x^2} + \frac{\partial^2 u}{\partial y^2} = \frac{1}{h^2}(u_{i+1,j} + u_{i-1,j} + u_{i,j+1} + u_{i,j-1} - 4u_{i,j}) \quad (6)$$

We can show that this second derivative value is closely related to a variation of the differencing algorithm. An average of absolute differences with surrounding traces in the differencing algorithm would consider:

$$d_{i,j} = (|u_{i+1,j} - u_{i,j}| + |u_{i-1,j} - u_{i,j}| + |u_{i,j+1} - u_{i,j}| + |u_{i,j-1} - u_{i,j}|) \quad (7)$$

By comparing the previous two equations, we see that the differencing expression for the second derivative map would be equivalent to the expression for the average absolute differences, d_{ij} , if all the quantities within the absolute value signs of d_{ij} were positive. Therefore, it is not surprising that our differencing and second derivative maps have a somewhat similar appearance. Also, both the differencing and second derivative measures generally have a higher frequency content than the C1 coherency algorithm since, in the Fourier domain, differentiation will multiply the Fourier transformed wavefield by spatial frequency while producing a 90 degree phase shift.

FAULT MAPPING

The quality of fault detection images depends on the quality of the input seismic data (Marfurt et al., 1998). In order to accurately image faults in a spatial sense, it is essential to apply our algorithms to depth migrated data. That is, in order to obtain faults as discontinuous features, they have to be properly migrated into their correct subsurface location. Undermigrated faults will produce diffractions and will be relatively coherent events.

This is illustrated by the simple fault model in Figure 3. This figure illustrates a simple extensional fault model, which consists of two stratigraphic layers with velocity $v_1 = 2500$ m/s and $v_2 = 3500$ m/s. The extensional fault had a throw of 400m and is at vertical position 1000m to 1400m.

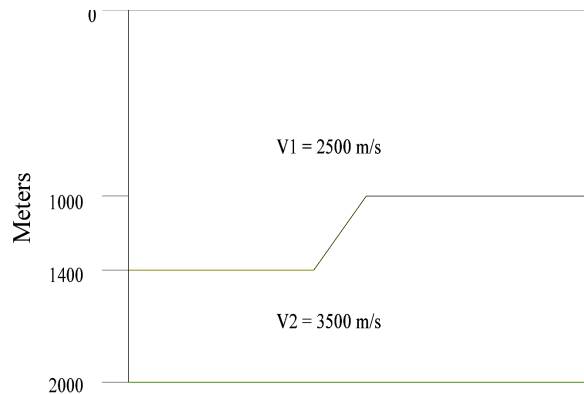


Figure 3. Simple fault model.

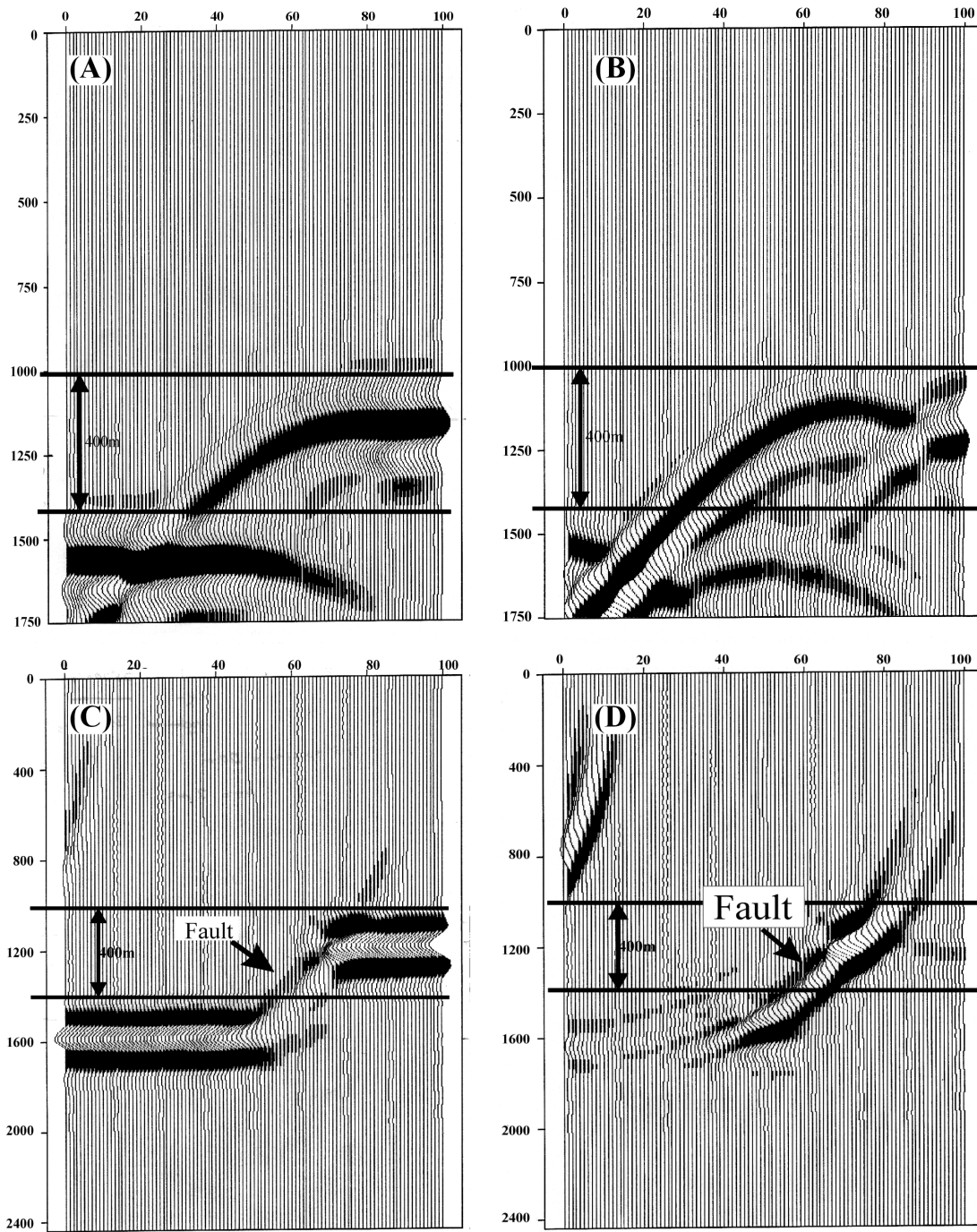


Figure 4. Differencing results of unmigrated and migrated data of the simple fault model: (A) unmigrated result, (B) differencing result of unmigrated section, (C) migrated result, and (D) differencing result of migrated section.

The fault model was used to create an “exploding reflector” synthetic seismogram, which represents an ideal stacked section, as shown in Figure 4a. This seismogram has considerable diffraction energy, which obscures the fault position. Figure 4b illustrates the differencing result of the unmigrated data as compared to the input data. For the unmigrated data, the differencing algorithm did not produce a result that defined the correct position of the fault.

Figure 4c shows a reverse time migration of the synthetic seismogram in which the fault’s position is more clearly defined. An application of the differencing algorithm clearly outlines the position of the fault, as shown by Figure 4d.

HIBERNIA DATA EXAMPLES

Both synthetic and real data sets used in this study are taken from Kelly (1998). The seismic data set used was a three-dimensional survey over the Hibernia field and a small portion of this 1991 survey was used to generate a model for the synthetic seismic data (Figure 5). The model data consisted of seven layers and the Murre fault and consists of 180 x-points, 132 y-points, and 333 z-points. This data was then poststacked depth migrated to obtain the optimum image. A slice then taken at the 215th depth sample was used for fault imaging using coherency and differencing techniques. The result of this comparison is shown in Figure 6a-d. A depth slice of the model data, which are input into the “fault enhancement” methods, is shown in Figure 6a. The C1 result is shown in Figure 6b, the result of the differencing is shown in Figure 6c, and the second derivative map is shown in Figure 6d. In each figure, the known fault position for the model is shown by the dashed line. The C1 method tends to enhance the fault compared to the other data. The differencing method enhances the fault but has a high spatial frequency “jitter”. The second derivative mapping also tends to emphasize the fault but shows less amplitude contrast with other events in the depth slice.

For the real data example in Figures 7a-d, we make the same type of comparison and mark an interpreted fault position by a dashed line. Both the coherency C1 algorithm and the differencing method do a good job of enhancing the fault.

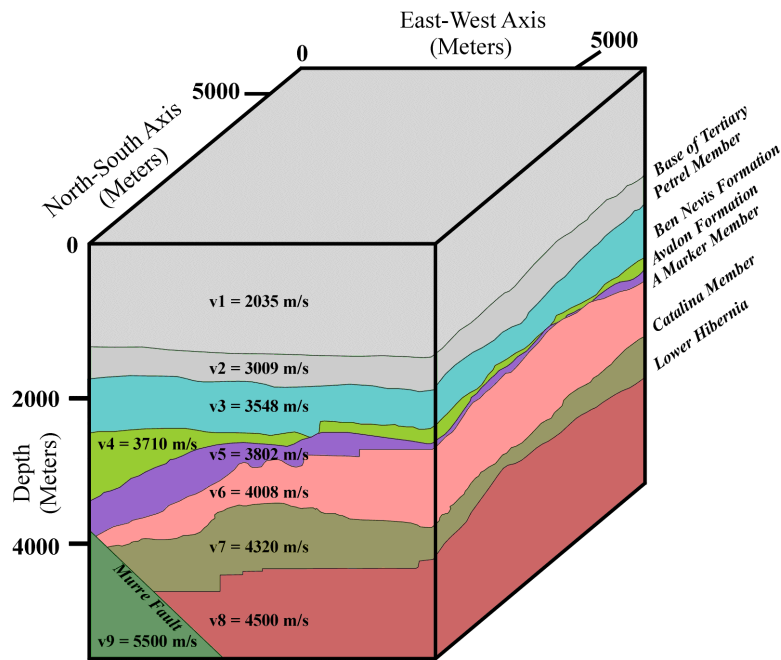


Figure 5. Complex Hibernia model (after Kelly, 1998).

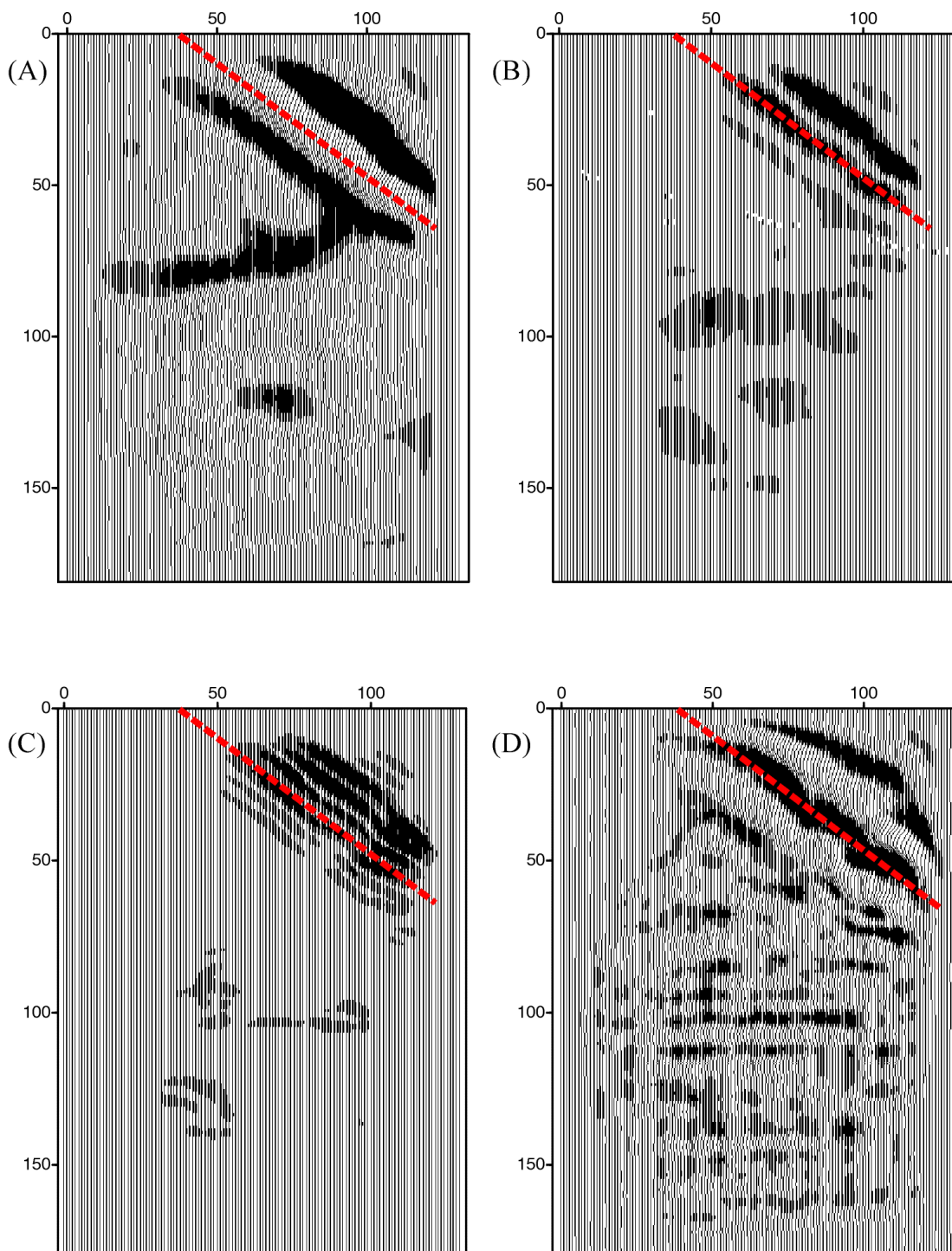


Figure 6. Comparison between coherence (B), differencing (C), and second derivative (D) result using input model (A) at depth slice 215 .

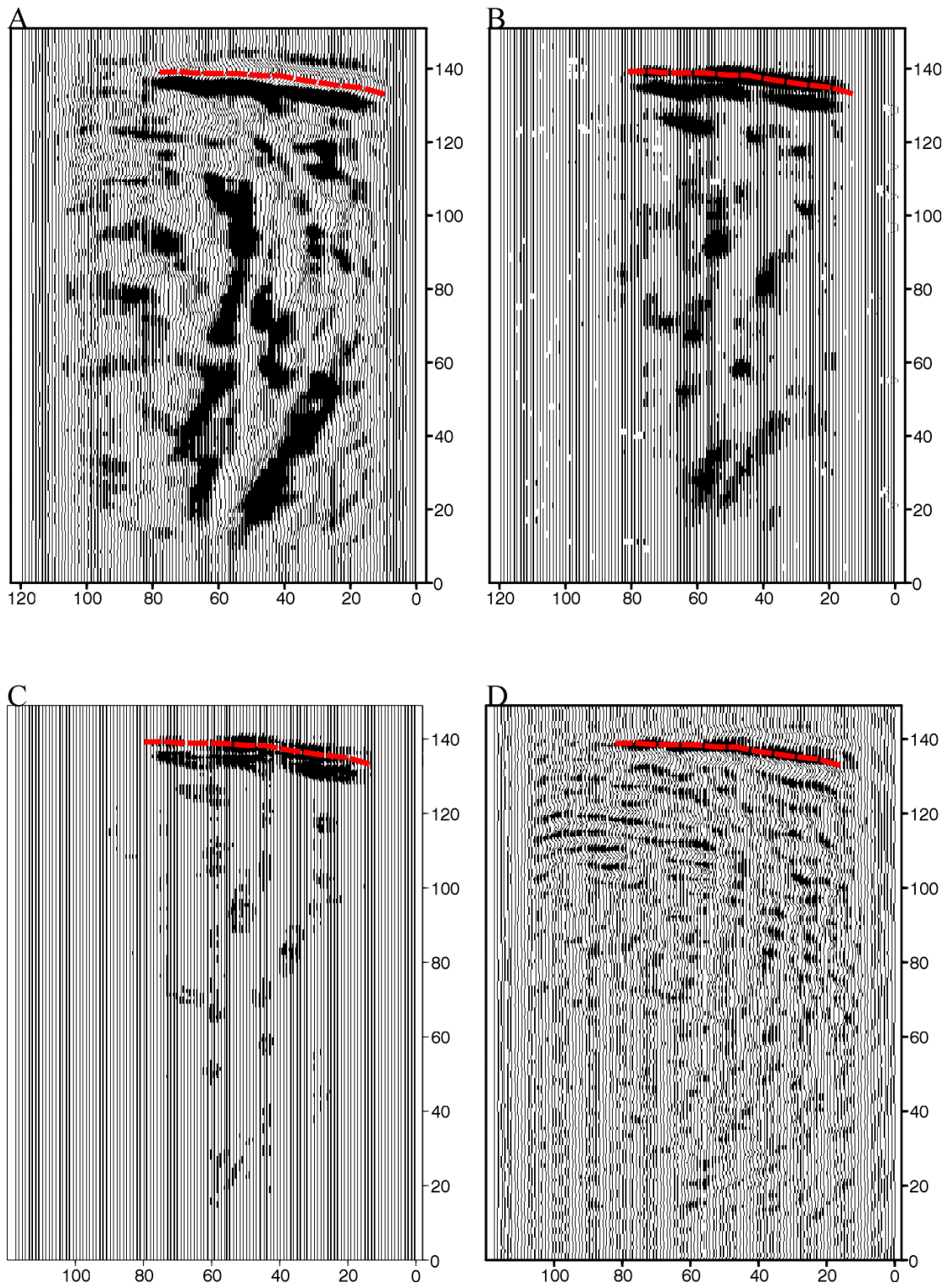


Figure 7. Comparison of result for depth slice 275. (A) input data, (B) coherency result, (C) differencing, and (D) second derivative result.

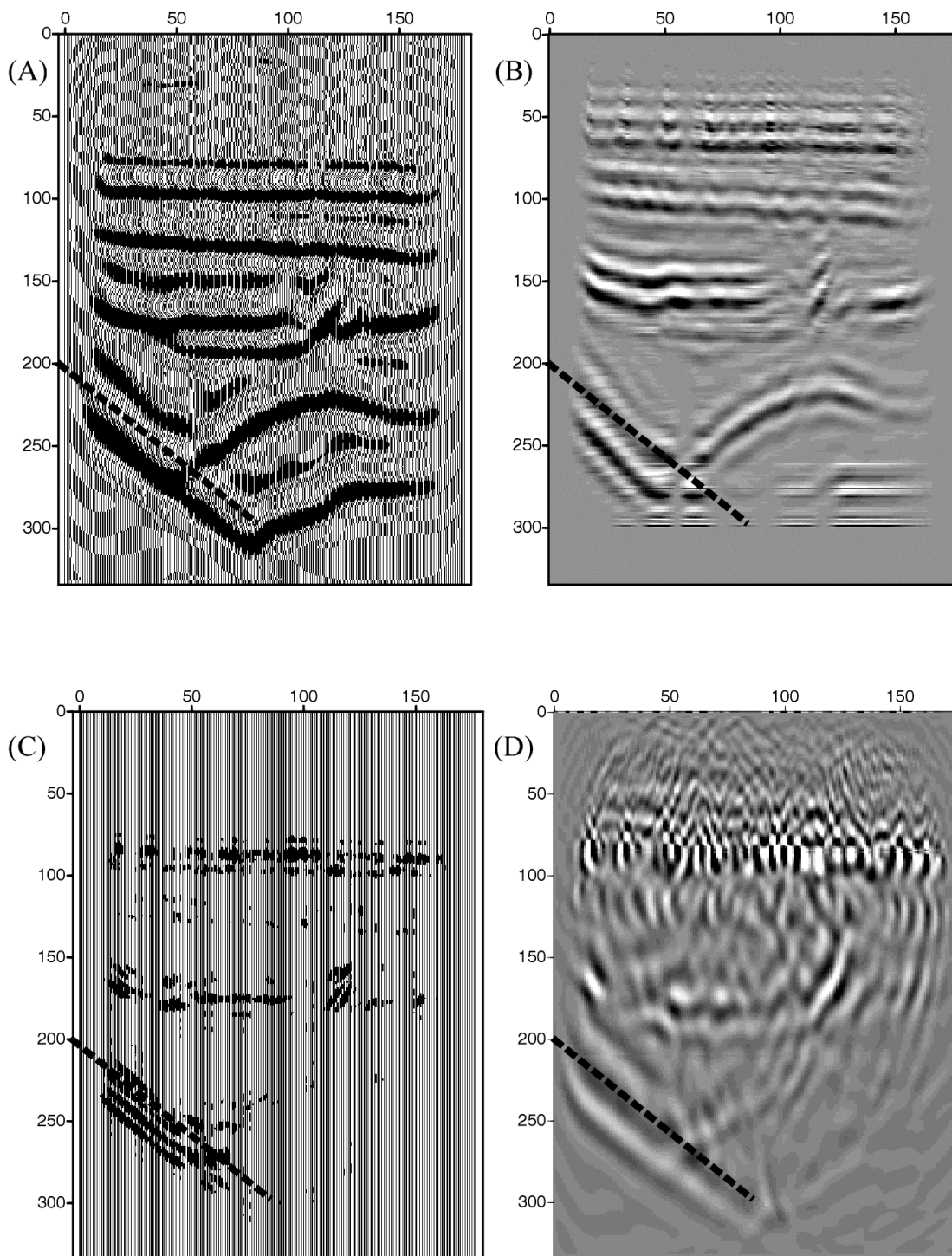


Figure 8. Comparison of results for in-line 60. (A) Input data, (B) coherency result, (C) differencing result, and (D) second derivative result.

The second derivative map does enhance the fault but once again shows less contrast between the fault and other events.

While we examined depth slices in map view in Figures 6 and 7, a comparison of the cross-sectional views of the Murre fault for the methods also proves interesting as shown in Figures 8a-d. Again, we note that all methods enhance the Murre fault relative to other reflections with the C1 algorithm and the differencing method doing better than the second derivative method. It should be noted that the estimate of the fault location can be displaced from its true location as shown by the dashed line on the model studies of Figure 6. This is effectively due to wavelet delay and can be cured by wavelet deconvolution. The delayed displacement of the Murre fault from its actual location is due to wavelet delay and can be remedied (or at least lessened) in the same manner as normal processing – by the use of wavelet deconvolution. The deconvolution can work effectively before or after edge enhancement – provided we have a reliable estimate of the wavelet and its delay characteristics.

CONCLUSIONS

The C1 coherency algorithm, the edge detection differencing method, and the second derivative method prove useful for detection of faults as exhibited by our experience with model and real data. Unlike the C1 algorithm, the differencing method and the second derivative method tend to produce high frequency oscillations. In terms of performance, the C1 and differencing algorithms outperformed the second derivative mapping in most cases. These techniques are valuable in mapping the extensional faulting in Hibernia field. In order to be effective, it is recommended that fault detection methods be applied to reliable depth migrations and that deconvolution be used to prevent wavelet delay.

ACKNOWLEDGMENTS

We thank Hibernia Management and Development Corporation (HMDC) for their contributions of models and data to this project. We are also grateful to the sponsors of the Memorial University Seismic Imaging Consortium (MUSIC) for their support. We thank Sven Treitel for encouraging us to write this paper for TLE. Finally, we thank Irene Kelly of PanCanadian Petroleum for providing a 3-D model and migrated data set for this study.

REFERENCES

- Bahorich, M.S. and Farmer, S.L., 1995, 3D seismic discontinuity for faults and stratigraphic features: the coherence cube: *The Leading Edge*, **14**, 10, 1053-1058.
- Carter, N., 1999, Fault imaging of Hibernia three-dimensional seismic data using edge detection and coherency measures: M.Sc. thesis, Memorial University of Newfoundland.
- Dobrin, M., Introduction to geophysical prospecting: Third edition, McGraw Hill.
- Gersztenkorn, A., and Marfurt, K.J., 1996, Eigenstructure based coherence optimization: 66th Ann. Internat. Mtg., Soc. Expl. Geophys., Expanded Abstracts, 328-321.

- Hurley, T.J., Kresia, R.D., Taylor, G.G., and Yates, W.R.L., 1992, The reservoir geology and geophysics of the Hibernia field, offshore Newfoundland, *in* Halbouty, M.T., Giant oil and gas fields of the decade, AAPG Memoir 54.
- Kelly, I.G., 1998, Modeling and migration of Hibernia seismic data: M.Sc. thesis, Memorial University of Newfoundland.
- Luo, Y., Higgs, W.G., and Kowalik, W.S., 1996, Edge detection and stratigraphic analysis using 3D seismic data: 66th Ann. Internat. Mtg., Soc. Expl. Geophys., Expanded Abstracts, 324-331.
- Marfurt, K.J., Kirlin, R.L., Farmer, S.L., and Bahorich, M.S., 1998, 3D seismic attributes using a semblance based coherency algorithm, *Geophysics*, 63, 1150-1165.
- Marfurt, K.J., Sudhaker, V., Gersztenkorn, A., Crawford, K.D. and Nissen, S.E., 1999, Coherency calculations in the presence of structural dip: *Geophysics*, **64**, 104-111.
- Nissen, S.E., Haskell, N.L., Steiner, C.T., and Cotterill, K.L., 1999, Debris flow outrunner blocks, glide tracks, and pressure ridges identified on the Nigerian continental slope using 3-D seismic coherency: *The Leading Edge*, **18**, No. 5, 595-599.